13th World Conference on Earthquake Engineering
Vancouver, B.C., Canada
August 1-6, 2004
Paper No. 3040

FRAGILITY CURVES FOR GRAVITY-TYPE QUAY WALLS BASED ON EFFECTIVE STRESS ANALYSES

Koji ICHII[1]

SUMMARY

Recent development of effective stress-based FEM analysis has enables seismic performance assessment of gravity-type quay walls for various geotechnical conditions. However, with these performance assessments using FEM, it is only possible to estimate the degree of deformation in a deterministic way, and another probabilistic procedure like the fragility curve approach is preferable in some case. This paper presents fragility-curves for gravity-type quay walls, which consider various design conditions including liquefaction resistance of foundations, based on results of FEM analyses.

A simple chart for seismic performance evaluation of gravity-type quay walls was proposed based on parametric study with an effective stress-based FEM. The chart can consider the effect of design seismic coefficient, liquefaction resistances of backfill and foundation soils, and depth of foundation layer. The applicability of the chart was verified with case histories. The results indicated that the chart could evaluate a wide range of displacement of quay walls, ranging from displacements in the order of one-tenth of meters to those one order higher, with an accuracy of twice or half order.

A damage level index based on the magnitude of seaward displacement for gravity-type quay wall was proposed based on restoration cost case histories. Considering the difference between the observed displacements in case histories and estimated displacements by the chart, a procedure to generate fragility curves for each damage level of gravity-type quay walls was proposed. And, fragility curves, which can consider the effect of design seismic coefficient, liquefaction resistances of backfill and foundation soils, and depth of foundation layer, were proposed as well.

The proposed fragility curves are quite useful for many situations, such as in the assessment of restoration cost after an earthquake, in the real-time damage level evaluation, and in the optimization of required seismic performance level based on cost-benefit analysis.

INTRODUCTION

Performance-based seismic design is an important aspect of the scope of seismic design discussed eagerly in the field of earthquake engineering. The performance-based design approach is expected to show how to mitigate a seismic disaster due to extremely strong earthshaking. Although the definition of the performance-based design is still controversial, the combination of a multi-level seismic intensity definition and a multi-level performance objective definition is utilized here to express this concept. SEAOC (Structural Engineers Association of California) introduced in Vision 2000 the recommended minimum seismic performance design objective for buildings in terms of the performance matrix[1]. For port structures, PIANC (International Navigation Association) introduced

[1] Senior Researcher, Port and Airport Research Institute, Japan

the performance-based methodology in its seismic design guideline.[2] These guidelines summarized the concept of performance-based design and the procedure for its application. However, these merely stated the conceptual methodologies and explained only a limited number of case histories.

Technical problems to be solved still remain such as:

- How to define the multi-level seismic intensity appropriately
- How to define the multi-level seismic performance objective appropriately
- How to evaluate the seismic performance of the structure
- How to handle the uncertainty of seismic performance evaluation

The first and the second problems should be considered in the context of seismic hazard mitigation planning. Since these are not only technical but also social and economic problems, engineers need to discuss the expected functions of structures during and after earthquakes based on the knowledge of the seismicity of the site.

The third problem is a purely technical problem and numerous engineers and researchers have been working on this issue. Many kinds of advanced technique including FEM (Finite element method), FDM (Finite difference method), DEM (Distinct element method) have been proposed. The applicability of these methods has been verified with case histories and experiments.

However, no matter how much the applicability of these advance methods has been increased by advanced modeling and verified with case histories, some amount of uncertainty still remains as to the results of these advanced techniques.

The fourth problem stands on the viewpoint of assessing uncertainties of the advanced method. It indicates that some probabilistic approach should be developed for decision-making in the design process.

Fragility curve approach is a simple but powerful tool for this issue. It is a tool to evaluate the failure probability of a structure for a corresponding seismic intensity level. Many curves have been proposed for a variety of structures [3][4]. A new method of making fragility curves by the combination of FEM and case histories is proposed in this paper resulting in a set of fragility curves for gravity-type quay walls.

SEISMIC PERFORMANCE CRITERIA FOR GRAVITY-TYPE QUAY WALLS

Gravity-type quay walls are made of a concrete caisson or other retaining structure placed on a foundation, sustaining earth pressures from backfill soil behind the wall. A concrete caisson wall is typically utilized for large-scale quay walls with -7.5m water depth or more. One prerequisite for maintaining the stability of the caisson-type quay wall is that the foundation soil beneath the caisson has sufficient bearing capacity. Therefore, the foundation soil has been improved to satisfy the required bearing capacity with a sand replacement method in some cases.

When the level of earthquake-induced excitation exceeds the limiting condition considered in the seismic design the caisson wall will move toward the seaside causing settlement behind the wall. Tilting of the wall also will occur. Damages on the concrete caisson itself were not observed in most of the cases. Foundation rubble drifted toward the sea due to the settlement of the caisson wall into the rubble foundation. Thus, the typical failure mode of caisson walls is summarized schematically in Fig. 1..

The most severe damages for the function of the quay wall are 1) widening of span between crane legs, 2) settlement (gap) behind the wall and 3) settlement (cracks) of apron as shown in Fig. 2.. Although it is difficult to define or measure the damage extent of settlement behind the wall and settlement of apron, seaward displacement or normalized seaward displacement (displacement divided by the wall height) of caisson wall might be related to these damages. Since span widening between crane legs is also related to seaward displacement of caisson walls, the extent of seaward displacement or normalized seaward displacement might be considered as damage criteria from the viewpoint of quay wall performance.

Considering the viewpoint mentioned above, multi-level damage criteria have been proposed based on seismic loss. Restoration case histories and their costs after the Kobe Port disaster in 1995 and

Kushiro Port disaster in 1993 are examined for this purpose. Note that the choice of restoration method depends not only on the damage level but also on many factors including space restrictions.

The 36 case histories with restoration costs in Kobe Port after the 1995 Hyogoken-nanbu earthquake and in Kushiro Port after the 1993 Kushiro-oki earthquake are examined. Fig. 3. shows the rough estimation of restoration cost per unit length (per meter along the face line) against the seaward displacement and the normalized seaward displacement at the top of the wall. Since the restoration cost depends on many factors such as restoration period, quay wall scale, etc., no unique relation between damage level and restoration cost is identified. However, as a rough estimation, the author defines four levels of damage criteria as shown in Fig. 3. Note that the restoration costs in Fig. 3 are a very rough estimation and sometimes include retrofit costs such as liquefaction countermeasures after an earthquake. It implies that the economic loss might be overestimated. However, these costs do not include indirect loss such as the economic impact on society, which in turn implies that the economic loss in this research might be underestimated. Although these points are left for future research, the author has defined these multi-level damage criteria for the following fragility curve generation.

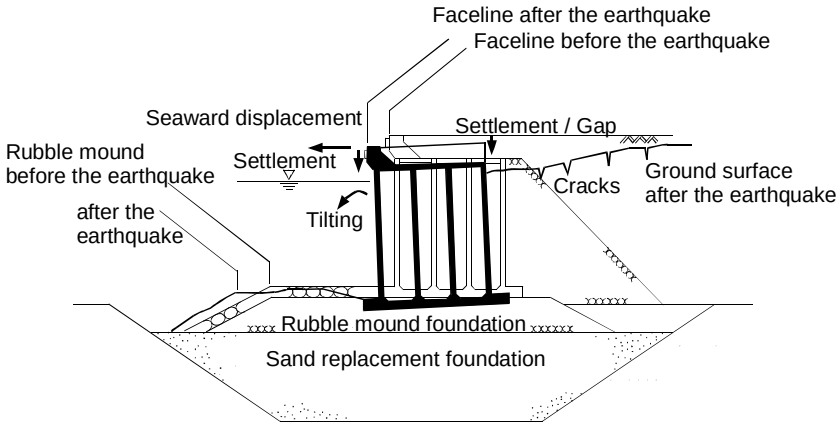

Fig. 1 A typical failure mode of a caisson-type quay wall due to earthquake

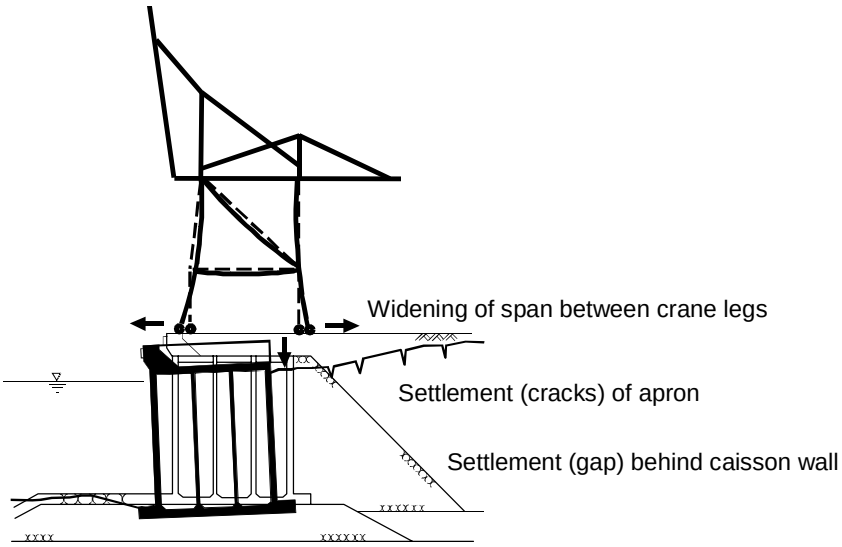

Fig. 2 Severe damages for the function of a quay wall

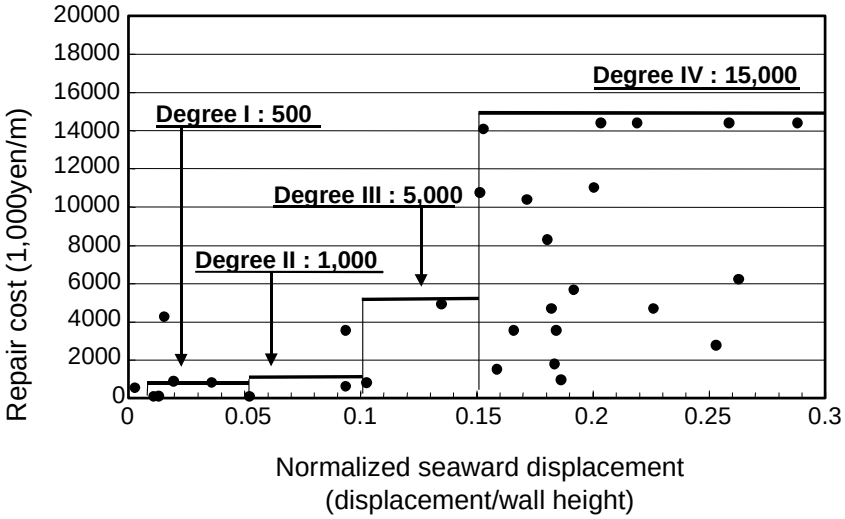

Fig. 3 Proposed damage criteria based on restoration cost

SEISMIC PERFORMANCE EVALUATION BY A FEM

Outline of the FEM code: FLIP

As one of the most advanced methods for seismic performance evaluation, the finite element method has been proposed. Details of the procedure of adapting finite element analysis to a dynamic problem have been discussed and summarized in textbooks.(e.g.[5])

To apply the finite element method on a structure with foundations, it is necessary to model the non-linear behavior of foundation materials. In addition, modeling of the excess pore water pressure buildup in sand is also important, since most of the damaged quay walls have suffered from the effect of liquefaction in their foundations and/or backfills.

The strain space plasticity model developed by Iai et al.[6] has been used for the seismic performance evaluation of many type of port structures.[7] This is a multiple mechanism model defined in strain space and can take the effect of principal stress axis rotation into account, which is known to play an important role in the cyclic behavior of sand under anisotropic stress conditions.[8] The computer code named FLIP (Finite element analysis of LIquefaction Process) with this constitutive model was used for this study.

Analysis of a quay wall on liquefiable soil

Most of the quay walls at Kobe Port were caisson type, constructed on loose saturated decomposed granite which was used to replace the alluvial clay layer in order to attain the required bearing capacity of the foundation. These walls moved about 5 m maximum, about 3 m on average, toward the sea in the 1995 Hyogoken-nanbu earthquake. The walls also settled about 1 to 2 m and tilted about 4 degrees toward the sea. There was little evidence of liquefaction of the backfill in the vicinity of the caisson walls whereas extensive evidence of liquefaction of landfill soil was observed inland about 30 m or further from the walls.[9]

Although the sliding mechanism could explain the large horizontal displacement of the caisson walls, this mechanism does not explain the large settlement and tilting of the caissons. On the other hand, the computed residual deformation after shakings is shown in Fig. 4.[7] As shown in this figure, the computed residual horizontal displacement and settlement at the top of the wall are about 3.5 m and 1.5 m, respectively. The tilting of the caisson wall is 4 degrees toward the sea. Thus, the computed deformation is consistent with the observation. The computed mode of the caisson wall is to tilt into and push out the foundation soil beneath the caisson, and it is also consistent with the observed deformation of rubble foundation measured by divers after the earthquake. Note that the accuracy of

the numerical simulation is fairly dependent on the technique and availability of information for both modeling and parameter calibration. This case was a particularly fortunate case as it was possible to do both detailed modeling and accurate parameter calibration.

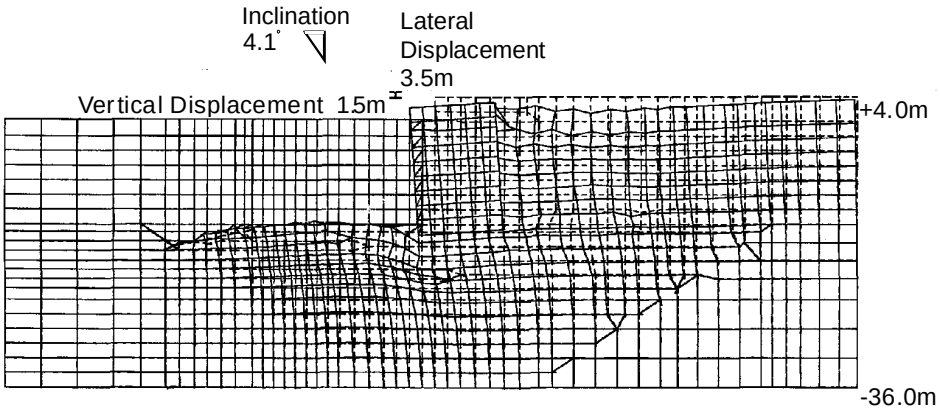

Fig. 4 Computed deformation of a quay wall at the end of shaking

SEISMIC PERFORMANCE EVALUATION CHARTS

Limitation of the advanced and empirical methods

Although the applicability of the effective stress analysis method for seismic performance evaluation of caisson-type quay walls was verified with case histories, it is difficult to conduct effective stress analyses for all varieties of quay walls considered during the design procedure due to the limitation of costs and time. Furthermore, the effective stress method needs many input parameters and the calibration of which is not easy. It is necessary to become accustomed with the program in advance if one wants to use, and practicing the parameter calibration and executing the numerical simulation is time-consuming. Even for a skilled engineer, it is easy to make mistakes in the calibration of parameters, and what is worse -- it is possible to cheat on the simulation results for political or other reasons. Therefore, it is desirable to establish a simple but robust estimation technique for deformation of quay walls and to confirm the numerical results in some cases.

For gravity-type quay walls, a conservative relation between seismic coefficients and the level of input motion needed to cause damage to quay walls was proposed based on the case histories.[10] Furthermore, a simplified damage evaluation technique using seismic coefficients was developed.[11] However, these studies are only applicable in the cases without liquefaction and it is difficult to take into account the effect of subsoil conditions below and behind quay walls. The applicability of the sliding block concept for this purpose was examined[12]; however, experimental results revealed the complexity of the behavior of caisson walls, and the sliding block concept does not work well for such a complex behavior.

To overcome this problem, simplified seismic performance evaluation charts based on parametric studies using effective stress analyses are proposed.

Parametric study using a structurally simplified model

Parameters characterizing caisson walls

The factors governing the seismic performance of a caisson-type quay wall include wall dimensions, the thickness of the soil deposit below the wall and liquefaction resistances of subsoil below and behind the wall, as well as the levels of seismic shaking at the base layer. In this study, the soil deposit below the wall was represented by a sand backfill used to replace the original soft clay deposit in order to attain the required bearing capacity. The effects of this soil deposit on the deformation of a caisson-type quay wall may be approximately the same as those of a natural sand deposit below the wall; thus,

the results of the parametric study may be applicable not only for the quay wall with sand replacement studied here but also for a quay wall constructed on a natural sandy deposit.

The standard cross section used for the parametric study is shown in Fig. 5. Major cross-sectional dimensions were specified by the width (W) and the height (H) of the caisson wall and by the thickness of subsoil (D1). For simplicity, the thickness of backfill (D2) was assumed to be the same as the wall height (H). A width-to-height ratio of the caisson wall (aspect ratio; W/H) is one of the most important parameters in conventional seismic design and correlates with the seismic coefficients used in the pseudo-static method as shown in Fig. 6, which is based on Japanese case histories. The width-to-height ratio (W/H) was thus considered a major parameter in this study. The parameters used in this study were W/H = 0.65, 0.90, 1.05, which correspond to the seismic coefficients of Kh = 0.1, 0.2, 0.25, respectively.

The peak accelerations of the input seismic excitation assigned at the base layer as the incident wave (as of 2E) ranged from 0.1 to 0.6 g. The time history of the earthquake excitation was that of the incident wave (2E) at the Port Island (Kobe) vertical seismic array site at a depth of –79m. Fig. 7 shows this time history, often used in Japan for evaluating seismic performance of high-seismic-resistance quay walls under Level 2 earthquake motions.

The thickness of the soil deposit below the wall (D1) was specified by a ratio with respect to the wall height (H), ranging from D1/H = 0.0 (i.e. a rigid base layer located immediately below the wall) to D1/H = 1.0 (i.e. thick soil deposit below the wall).

Other geometrical conditions assumed for the effective stress analyses include: wall height H = 13m, water level = 2m lower than the top of the wall, thickness of the rubble mound = 4m.

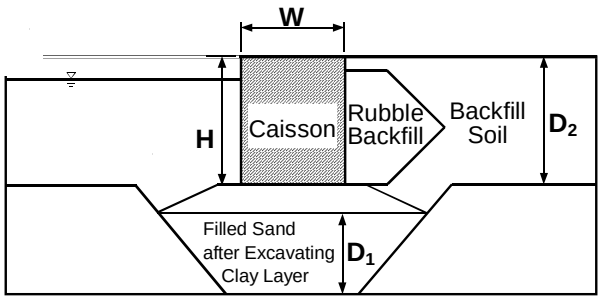

Fig. 5 Typical cross section of a gravity-type quay wall for parametric study

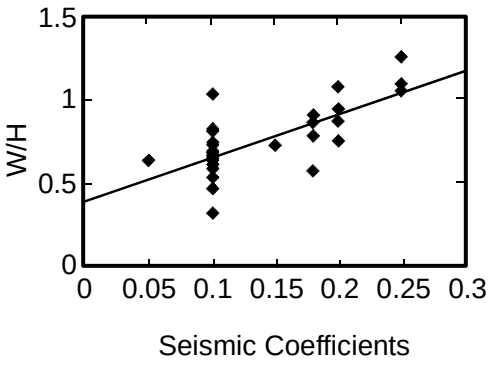

Fig. 6 Correlation between the width-to-height ratio (*W/H*) and seismic coefficients

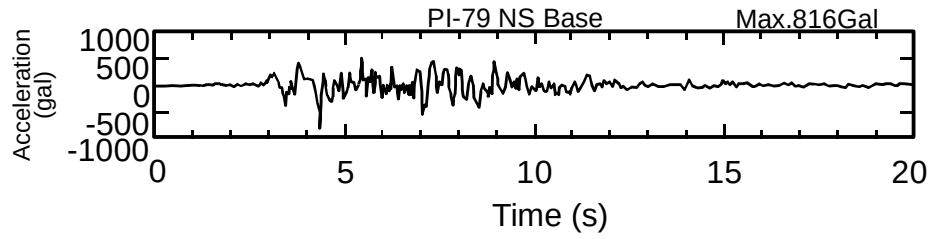

Fig. 7 Time history of input ground acceleration (2E)

Geotechnical conditions and parameters

For simplicity, the geotechnical conditions of the soil deposits below and behind the wall were assumed to be the same, represented by the equivalent SPT N value (the corrected SPT N value for the effective vertical stress of 65 kPa in terms of an equivalent relative density). The equivalent SPT N value has been widely used for the assessment of liquefaction potential in Japanese port areas.[13] Model parameters were determined by the equivalent SPT N values based on a simplified procedure.[14] The geotechnical model parameters determined by the equivalent SPT N values are summarized in Table 2. The assumed relative density (Dr) for each equivalent SPT N value, which was given in the process of the simplified procedure, is also shown in Table 1 as a reference.

Finite element modeling

An example of FEM mesh before and after the deformation is shown in Fig. 8. Four types of elements were used in the analyses: linear elements for the caisson, nonlinear elements for sand and clay, liquid elements for the seawater and joint elements for the boundaries between soil and structure. The input earthquake motion was specified at the bottom boundary through equivalent viscous dampers to simulate an incident transmitting wave (i.e. 2E).

PARAMETER SENSITIVITY AND CHARTS

The results of the parametric study were summarized in terms of the residual horizontal displacement (d) at the top of the wall. The residual horizontal displacement was normalized with respect to the wall height (H). The effects of the major parameters on the normalized residual horizontal displacement (d/H) are discussed as follows.

Width-to-Height Ratio (W/H)

The effects of width-to-height ratio (W/H) on the displacement are shown in Fig. 9 for the equivalent SPT N value of 15. When the foundation below the wall is rigid (i.e. D1/H = 0), increasing W/H reduces the wall displacement. However, when the foundation soil is medium to dense (i.e. with the equivalent SPT N values of 15) and thick (i.e. D1/H = 1.0), the effects of W/H become less obvious.

Input Excitation Level

The effects of input excitation level are shown in Fig. 10 for W/H = 0.9, which corresponds to the seismic coefficient of Kh = 0.2 (see Fig. 10). Except for the equivalent SPT N values of 5 and 8, at which extensive liquefaction significantly increases the displacement, the normalized displacements for the excitation of 0.2 g at the base layer are within d/H < 0.03. The horizontal displacement of a wall for d/H = 0.03 is, for example, 0.3 m for a quay wall with H = 10 m, suggesting that the quay wall designed with a seismic coefficient of 0.2 based on the conventional pseudo-static method withstands the excitation of 0.2 g at the base layer if a margin of displacement in the order of 0.3 m is allowed.

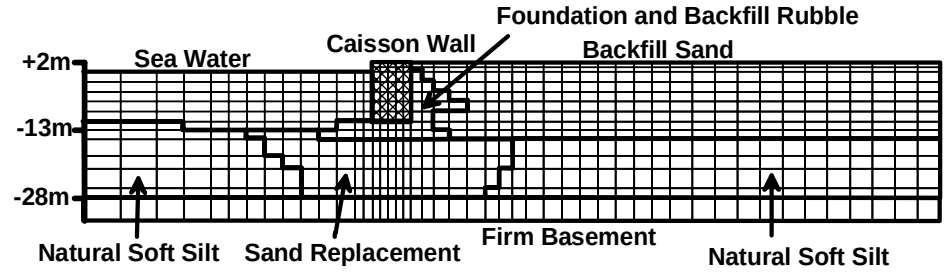

(a) An example of FEM Mesh and Material Configuration

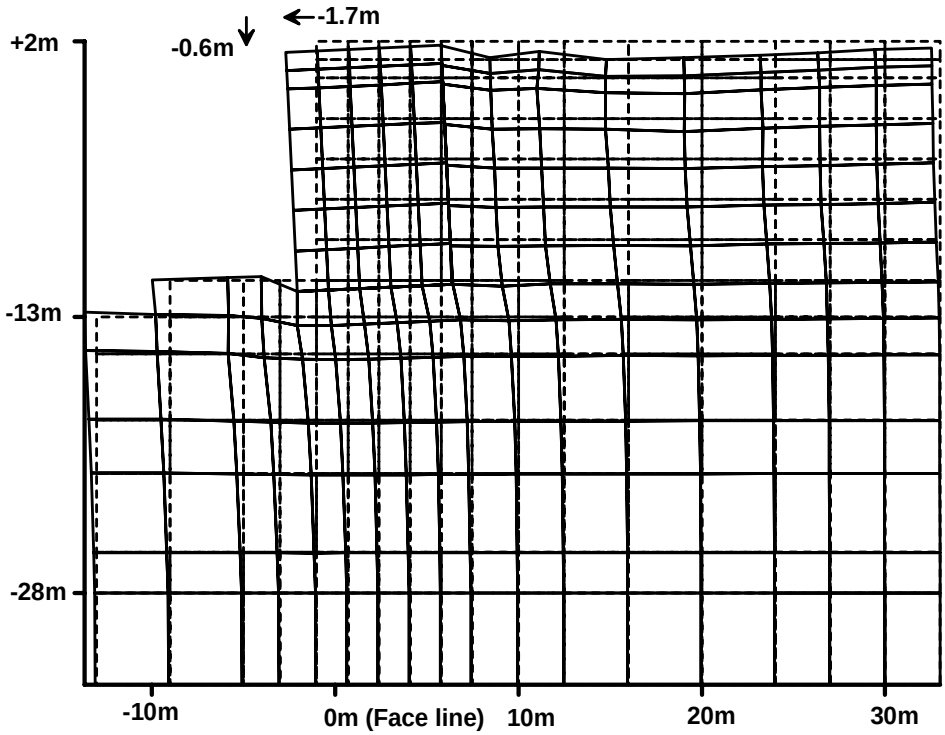

(b) An example of deformation around caisson wall

Fig. 8 An example of FEM mesh (*W/H* = 0.65, *D1/H* = 1.0)

Equivalent SPT N value

The effects of the equivalent SPT N value are shown in Fig. 11 for W/H = 0.9. Obviously, the thickness of the soil deposit below the wall significantly affects the displacement. For a wall built on a rigid foundation (D1/H = 0), the effects of the equivalent SPT N value of soil behind the wall are relatively small. For a wall built on a thick soil deposit (D1/H = 1.0), the effects of the equivalent SPT N values of the soil below and behind the wall are significant.

Thickness of Soil Deposit Below Wall

The effects of the thickness of the soil deposit below the wall are shown in Fig. 12 for W/H = 0.9. When the level of excitation is high, significant increase in the displacement is recognized for D1/H < 0.5 and for smaller SPT N values, suggesting that the existence of a soil deposit below the wall and its SPT N values are two important factors that affect the displacement.

Procedures for evaluating wall displacement

Based on the results of the parametric study shown in the previous section, a simple procedure is easily developed for evaluating the displacement of gravity-type quay walls. In this procedure, the

displacement is evaluated with respect to the parameters in the order of their sensitivity to the displacement. First, a rough estimation is given by Figs. 10 or 11. Since these two figures show identical results, only in a different manner, whichever is easier to read can be applied. Next, the correction for D1/H is applied based on Fig. 12. Finally, the estimation is given after the correction for W/H based on Fig. 9. However, the scale effects are not yet examined as mentioned above. Thus, the applicability of Figs. 9 to 12 might only be valid for the quay wall with large water depth (i.e. H = approx. 13m).

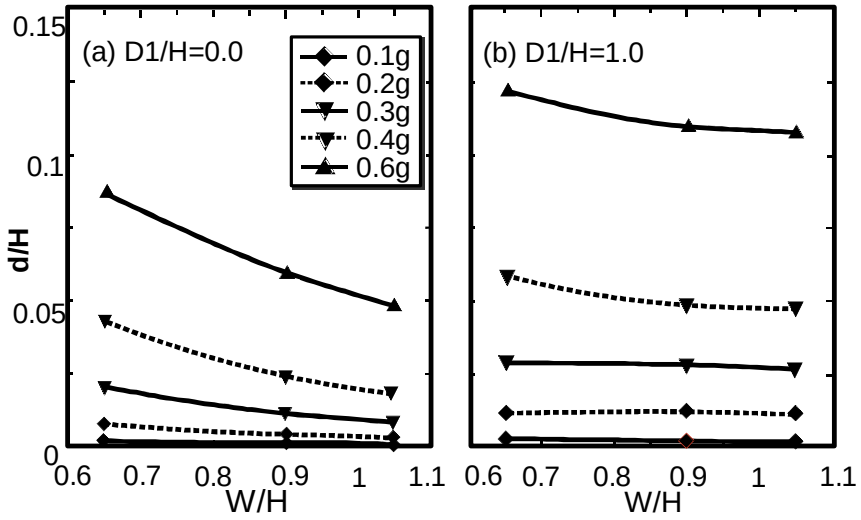

Fig. 9 Effects of the width-to-height ratio *W/H* (for equivalent SPT N value of 15)

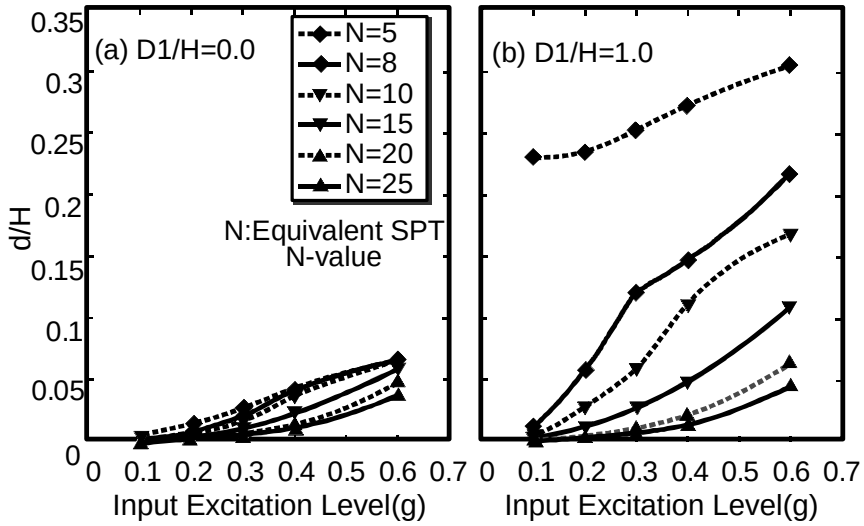

Fig. 10 Effects of the input excitation level (for *W/H* = 0.9)

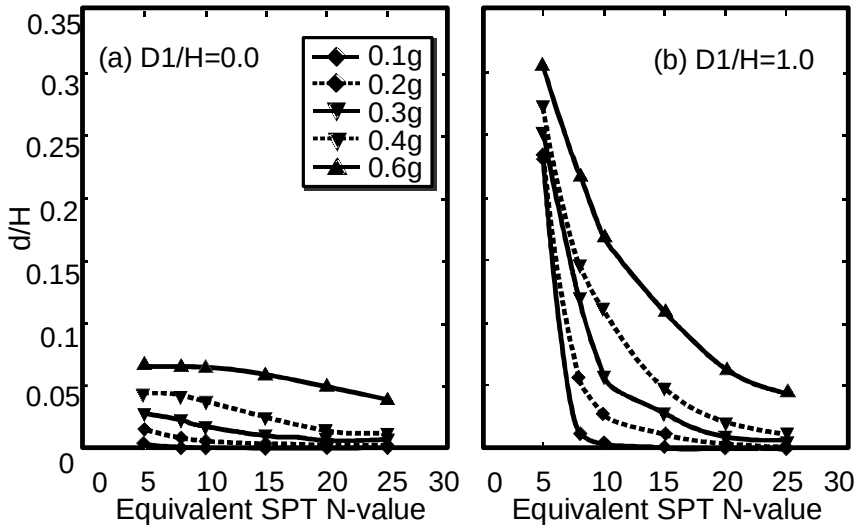

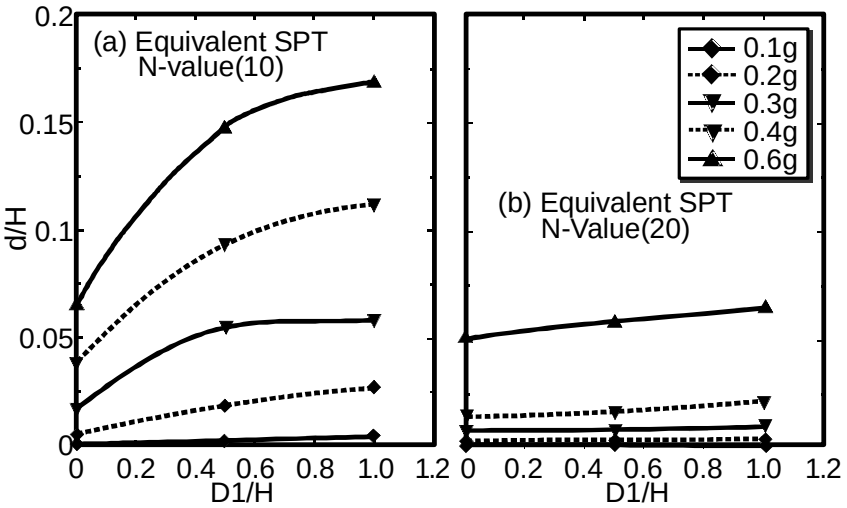

Fig. 12 Effects of thickness of soil deposit below the wall (for *W/H* = 0.9)

Table 1 Geotechnical model parameters for parametric study

Equivalent STP N values	G_{ma} (kPa)	σ'_{ma} (kPa)	ϕ_f (degree)	ϕ_p (degree)	p1	p2	w1	S1	c1	Dr (%)
5	56100	98.0	39.0	28.0	0.5	1.12	1.15	0.005	1.6	41
8	73380	98.0	39.6	28.0	0.5	1.06	3.76	0.005	1.6	48
10	84900	98.0	40.0	28.0	0.5	1.02	5.5	0.005	1.3	55
15	108000	98.0	41.0	28.0	0.5	0.92	9.2	0.005	1.3	66
20	132000	98.0	42.0	28.0	0.5	0.8	23.5	0.005	1.0	77
25	152000	98.0	42.0	28.0	0.5	0.7	50.0	0.005	1.0	85

FRAGILITY CURVE BASED ON THE COMBINATION OF FEM AND CASE HISTORIES

The fragility curve is a widely practiced approach to evaluate the seismic vulnerability of structures in terms of probability. [3][4] In the fragility curve approach, it is assumed that the curve is expressed in the form of two parameter lognormal distribution functions. Thus, the estimation of the two parameters (median and log-standard deviation) is carried out with the maximum likelihood method. The likelihood function for the present purpose is expressed as follows.

$$L = \prod_{i=1}^{N} [f(a_i)]^{x_i} [1 - f(a_i)]^{1-x_i} \tag{1}$$

Where $F(\cdot)$ represents the probability of occurrence for the specific state of damage; a_i is the peak input acceleration, commonly referred to as PGA which is the peak basement acceleration in terms of rock outcrop motion (2E) as used in this paper; x_i =1 or 0 for the case that the quay wall sustains the state of damage or not, respectively, under the current input excitation; and N is the total number of case histories. Under the current lognormal assumption, $F(a)$ takes the following analytical form:

$$F(a) = \Phi\left[\ln(a/c) \Big/ \zeta \right] \tag{2}$$

in which a represents the peak acceleration, and c and ζ in Eq. (2) are computed as c_e and ζ_e satisfying the following equations to maximize $\ln L$ and hence L :

$$\frac{d \ln L}{dc} = \frac{d \ln L}{d\zeta} = 0 \tag{3}$$

Since a straightforward algorithm can carry out this computation, the only remaining problem is how to collect or generate enough case histories considering all of the parameters that can be varied. Instead of gathering actual case histories, a simple technique with a random variable was adopted to generate case histories. The applicability of the proposed simplified seismic performance evaluation chart was examined again with 55 case histories from Kobe and Kushiro ports as shown in Fig. 13. Though some cases yield more than twice the observed values while other cases yield less than half of the observed values, there is good agreement in general. Based on linear regression analysis of these results for the condition that the regression curve go through the origin, a correction factor of $\hat{b}_1 = 1.2997$ and standard error of $\hat{\sigma} = 0.10914$ are obtained for the following equation.

$$d/H_{\_observed} = b_1 (d/H_{\_estimated}) + \varepsilon \tag{4}$$

Using these values, 1000 samples of case histories were artificially generated with the following procedure for a specific condition.

1) Produce 1000 samples of input acceleration levels in the range of 100 to 600 cm/s^2 with a uniform distribution.
2) Obtain estimates of the damage for each input acceleration level for a specific condition based on the charts. Since the original numerical parametric study for charts was conducted on discrete values of 100, 200, 300, 400 and 600 cm/s^2, the estimation is given by linear interpolation with these values.
3) Apply Eq. (4) with a random error distribution to each estimation.
4) Finally, obtain 1000 damage case histories that consider the overall variability in a specific condition.

However, the error distribution for Eq. (4) is uniform regardless of the calibrated damage level. Therefore, the variability of generated case histories is relatively large for the small damage level. And a modification to Eq. (4) was carried out as,

$$d/H_{\_observed} = (b_1 + \varepsilon')(d/H_{\_estimated}) \quad (4)'$$

in which the correction factor $\hat{b}_1 = 1.2997$ is the same as before, but the standard error of $\hat{\sigma} = 1.05176$ is different.

Fig. 14 shows an example of 1000 case histories generated by the proposed technique with both Eqs. (4) and (4)' for the input of W/H = 0.9 (the aspect ratio of caisson wall), D1/H = 0.5 (the normalized depth of the sand deposit below the wall) and N65 = 10 (the equivalent SPT N value below and behind the caisson). Using Eq. (4), the generated results are scattered over a wide range regardless of input acceleration level. However, using Eq. (4)', the scattering of the generated results is much lower and the relationship between the results and the input acceleration level can be recognized. Thus, the procedure using Eq. (4)' can be regarded as the better procedure for risk assessment than the procedure with Eq. (4). It should be noted here that if the generated displacement is negative, it is regarded as zero damage for the sake of simplicity.

Table 2 Calibrated parameters of fragility curves

Equivalent SPT N	Aspect ratio (W/H)	Normalized thickness of sand deposit	Degree I		Degree II		Degree III		Degree IV	
			c	ζ	c	ζ	c	ζ	c	ζ
5	0.90	0.00	160.1	1.12	414.8	0.50	615.6	0.38	689.7	0.25
8	0.90	0.00	246.3	0.65	438.5	0.40	611.9	0.33	663.7	0.19
10	0.90	0.00	291.6	0.50	453.7	0.36	607.9	0.28	649.2	0.17
15	0.90	0.00	337.5	0.45	505.2	0.25	608.0	0.16	635.3	0.09
20	0.90	0.00	388.2	0.37	545.7	0.18	619.7	0.12	678.6	0.11
25	0.90	0.00	412.7	0.34	574.4	0.15	631.9	0.09	2650.1	0.29
5	0.90	1.00	0.1	7.05	0.1	8.27	0.1	9.39	0.2	11.68
8	0.90	1.00	11.3	3.27	146.3	1.17	276.9	0.79	366.7	0.65
10	0.90	1.00	93.6	1.40	268.1	0.65	390.1	0.46	462.6	0.39
15	0.90	1.00	209.6	0.75	392.5	0.42	511.0	0.29	589.9	0.22
20	0.90	1.00	353.1	0.41	506.6	0.23	600.5	0.16	617.7	0.08
25	0.90	1.00	404.9	0.33	560.5	0.19	617.1	0.10	1751.9	0.49
15	0.65	0.00	262.7	0.55	429.2	0.35	555.1	0.28	625.8	0.21
15	0.90	0.00	337.5	0.45	505.2	0.25	608.0	0.16	625.3	0.09
15	1.05	0.00	375.4	0.38	547.2	0.22	629.6	0.14	713.9	0.12
15	0.65	1.00	208.1	0.74	378.8	0.41	484.4	0.31	568.8	0.26
15	0.90	1.00	209.6	0.75	392.5	0.42	511.0	0.29	589.9	0.22
15	1.05	1.00	215.5	0.73	400.0	0.41	512.5	0.29	587.5	0.20
10	0.90	0.50	145.8	1.01	307.9	0.53	414.8	0.45	499.8	0.41
20	0.90	0.50	375.2	0.37	523.2	0.19	609.8	0.14	638.7	0.09

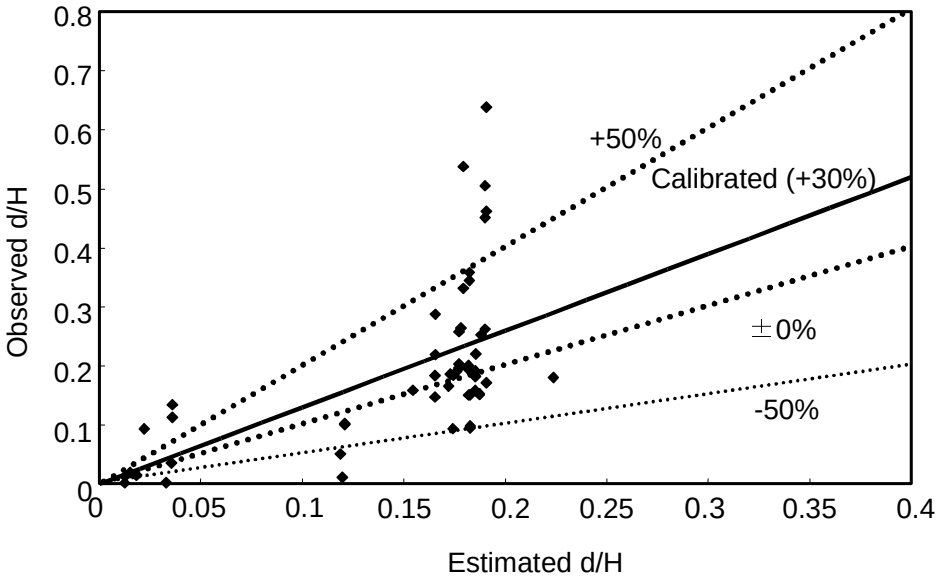

Fig. 13 Applicability verification results of the seismic performance evaluation charts

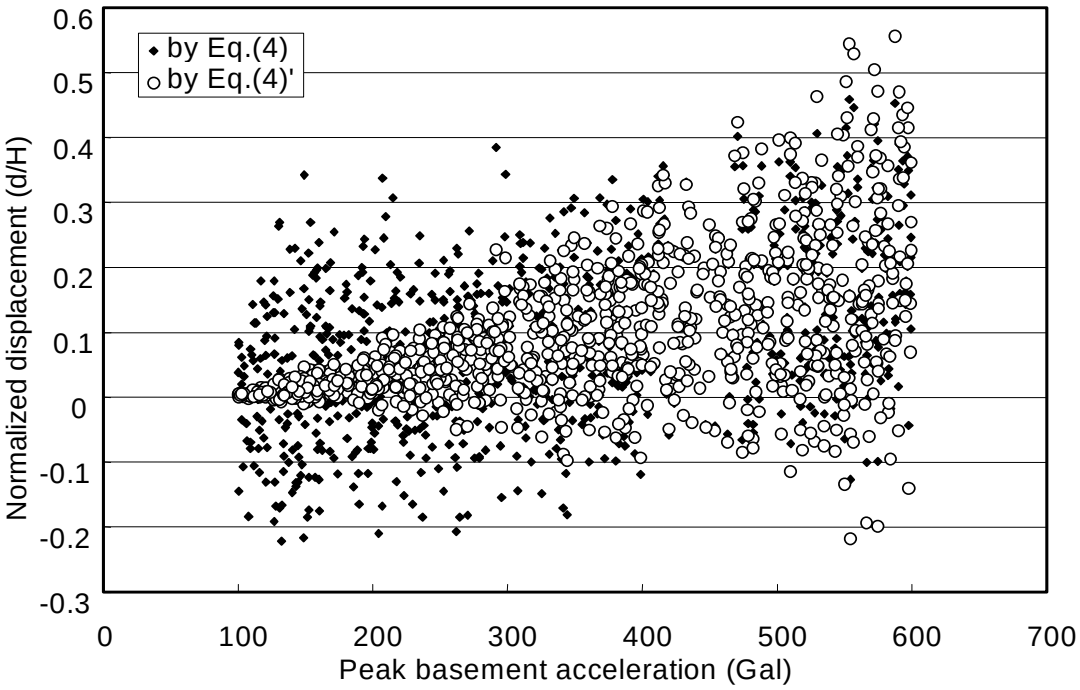

Fig. 14 Examples of generated case histories

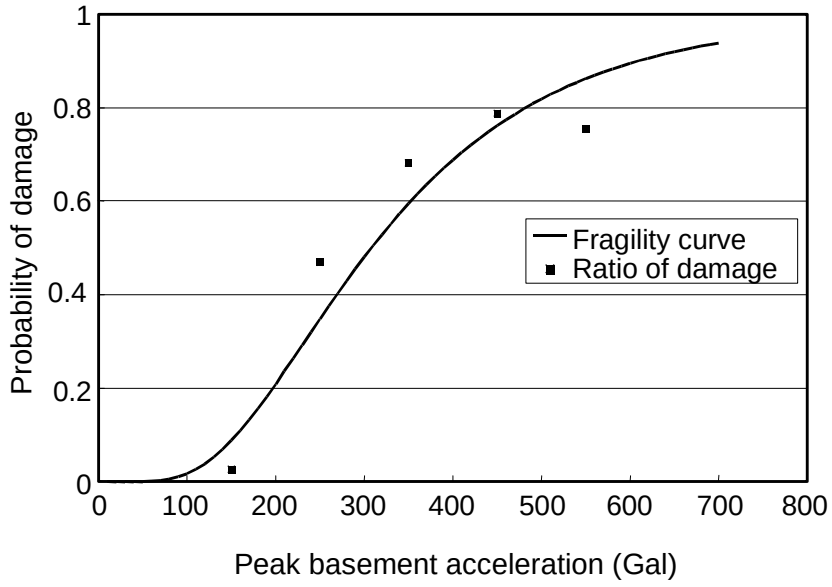

Fig. 15 An example of fragility curve generation

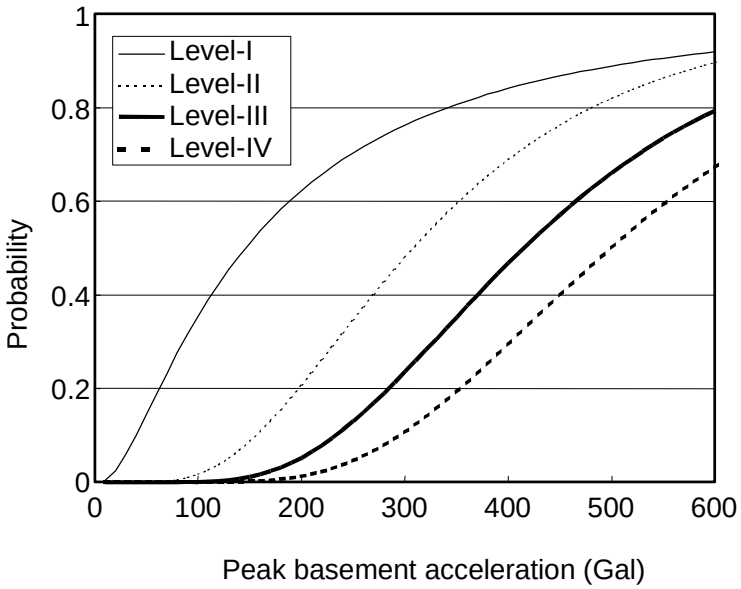

Fig. 16 Examples of generated fragility curves

An example of a fragility curve calibration is shown in Fig. 15, which is for the specific condition of W/H = 0.9, D1/H = 0.5, N65 = 10 and for damage level II. Since generated cases are too numerous, the damage ratios of generated cases for each 100 cm/s^2 are shown in this figure as a reference. Thus, the calibrated fragility curve shows good agreement with the generated case histories. As an example, the fragility curves for this condition are shown in Fig. 16. A summary of the calibrated parameters for each line in the evaluation charts is shown in Table 2.

DISCUSSION: APPLICATIONS OF THE FRAGILITY CURVES

Once the fragility curves for each specific condition are obtained, it is easy to produce the relationship between the loss and the input excitation level since damage criteria with their loss estimations were already proposed in Fig. 3. The product of the loss for each damage level shown and the probability of each damage level given by the fragility curve gives the estimated loss for each input excitation level. Thus, seismic risk assessment was enabled by the proposed fragility curves. These fragility curves can be applied for not only a seismic risk assessment but also other purposes such as a real-time seismic damage assessment.

Although the variety of the proposed fragility curves are limited, more detailed variation of curves can be calibrated if a more detailed parametric study were carried out. Thus, the proposed method for fragility curve calibration has a huge potential for future development.

Note the ground motion level for the proposed fragility curves are PGA at the basement layer and the wave characteristics are assumed to be equivalent with the observed motion in Kobe Port since all the parametric study is based on this specific motion. Therefore, the effect on the differences of ground motion characteristics should be investigated in future study.

CONCLUSIONS

A set of simple charts for seismic performance evaluation for gravity-type quay walls has been proposed based on parametric study with an effective stress-based FEM. Considering the difference between the observed displacements in case histories and estimated displacements by the chart, a procedure to generate fragility curves for each damage level of gravity-type quay walls were proposed. Since the chart can consider the effect of design seismic coefficient, liquefaction resistances of backfill and foundation soils, and depth of foundation layer, the proposed fragility curve also can consider these differences.

The proposed fragility curves are quite useful for many situations, such as in the assessment of restoration cost after an earthquake and in the real-time damage level evaluation. Although the variety of the proposed fragility curves are still limited, more detailed variation of curves can be calibrated if a more detailed parametric study were carried out. Thus, the proposed method for fragility curve calibration has a huge potential for future development.

REFERENCES

1 SEAOC, ”Vision 2000 - A Framework for Performance Based Design”, Volumes I, II, III, Structural Engineers Association of California, Vision 2000 Committee, Sacramento, California, 1995.

2 PIANC, ”Seismic design guidelines for port structures”, International Navigation Association, Balkema, 2001, 474p.

3 Shinozuka, M., Feng, M. Q., Lee, J. and Naganuma, T., “Statistical analysis of fragility curves, Journal of Engineering Mechanics”, ASCE, Vol. 126, No. 12, 2000, pp. 1224-1231.

4 Nakamura, T., Okada, K. and Honma, N., ”A study on slope failure probability by earthquake based on statistical method”, Journal of geotechnical engineering, JSCE, No. 570 / I-40, 1997, pp. 73-82. (in Japanese)

5 Zienkiewicz, O.C., “The Finite Element Method”, 3rd edition, McGraw-Hill Book Co., 1997.

6 Iai, S., Matsunaga, Y. and Kameoka, T., ”Strain space plasticity model for cyclic mobility”, Soils and Foundations, Vol.32, No. 2, 1992a, pp. 1-15.

7 Iai, S., ”Rigid and flexible retaining walls during Kobe earthquake”, Fourth International Conference on Case Histories in Geotechnical Engineering, Paper No. SOA-4, St.Louis, Missouri, 1998.

8 Iai, S., Matsunaga, Y. and Kameoka, T. , ”Analysis of undrained cyclic shear behavior of sand under anisotoropic consolidation”, Soils and Foundations, Vol. 32, No.2, 1992b, pp. 16-20.

9 Inagaki, H., Iai, S., Sugano, T., Yamazaki, H. and Inatomi, T., ” Performance of caisson type quay walls at Kobe Port”, Special issue of Soils and Foundations, Japanese Geotechnical Society, 1996, pp. 119-136.

10 Noda, S., Uwabe, T. and Chiba, T.,”Relation between seismic coefficient and ground acceleration for gravity quay wall”, Report of the Port and Harbour Research Institute, Vol. 14, No. 4, 1975.(in Japanese)

11 Uwabe, T., ”Estimation of earthquake damage deformation and cost of quay walls based on earthquake damage records”, Technical note of the Port and Harbour Research Institute, No. 473, 1983. (in Japanese)

12 Mohajeri, M., Ichii, K. and Tamura, T., ”Experimental Study on Sliding Block Concept for Caisson Walls”, Journal of Waterway, Port, Coastal and Ocean Engineering, ASCE, 2003. (in Printing)

13 PHRI, ”Handbook on Liquefaction Remediation of Reclaimed Land”, Port and Harbour Research Institute, A.A. Balkema, Rotterdam, Brookfield, 1997.

14 Morita. T., Iai, S., Liu, H., Ichii, K. and Sato, Y., ”Simplified method to determine parameter of FLIP”, Technical note of Port and Harbour Research Institute, No.869, 1997. (in Japanese)